

Multiple Higgs-Portal and Gauge-Kinetic Mixings

S. Y. CHOI¹, C. ENGLERT², AND P. M. ZERWAS³

¹ *Department of Physics, Chonbuk National University, Jeonju 561-756, Republic of Korea*

² *SUPA, School of Physics and Astronomy, University of Glasgow, Glasgow, G12 8QQ, United Kingdom*

³ *Theory Group, Deutsches Elektronen-Synchrotron DESY, D-22603 Hamburg, Germany*

(March 8, 2018)

We develop a phenomenological formalism for mixing effects between the Standard Model and hidden-sector fields, motivated by dark matter in the Universe as well as string theories. The scheme includes multiple Higgs-portal interactions in the scalar sector as well as multiple gauge-kinetic mixings in the abelian gauge sector. While some of the mixing effects can be cast in closed form, other elements can be controlled analytically only by means of perturbative expansions in the ratio of standard scales over large hidden scales. Higgs and vector-boson masses and mixings are illustrated numerically for characteristic processes.

1. BASICS

A large fraction of matter in the Universe is invisible [1]. This hidden sector may have structures at least as complex as matter and interactions in the visible Standard Model [SM] sector (see e.g. [2]), unlike one-component theories as realized in supersymmetry approaches to the dark sector. Opportunities to explore structures in this hidden sector are offered by mixing effects with fields of the SM. Couplings between the two sectors are provided by Higgs-portal interactions [3–7] and gauge-kinetic mixings [4, 8, 9]. Higgs-portal interactions couple the invariant bilinear product of the Higgs field in the Standard Model with Higgs SM-singlets in the hidden sector [HS], the strength of the interaction measured by η . Kinetic mixing couples abelian hypercharge B, V -field tensors in both sectors with strength s . The coupling η can be varied in the analysis in a large range [10], $|\eta| \leq 1$, and the kinetic coupling s in the most general scenario in a similar range $|s| \leq 1$, depending strongly however on the underlying microscopic picture of the mixing mechanism.¹ If in field-theoretic models loops of mediators link the hypercharge B, V fields in the two sectors, the size of $|s|$ is expected to be restricted to $|s| \sim g_{\text{SM}} g_{\text{DM}} / 6\pi^2 \times \text{mass logs} \lesssim 10^{-2}$, set in detail by the gauge couplings, the hypercharges and the masses [8]. On the other hand, the kinetic coupling as mediated by string states is less stringently restricted in general, and it can be quite large depending on the type of string theory realized, see e.g. [11]. We will not delve into building a detailed model of the joined [SM]⊕[HS] system, nor of dark-matter candidates. However, the HS system may be taken as a SM-type system [12], properly extended to accommodate the dark-matter properties. The lightest fermion field, among others, could be a stable candidate in such a scenario for

¹ We are very grateful to J. Jaeckel for valuable advice on field- and string-theoretic models of kinetic mixing and consequences for the potential range of $|s|$.

the dark-matter field. The hidden-sector scales will be assumed of TeV size, contrasting approaches in which fields are assumed super-light. The present analysis aims at exploring the potential of high energy colliders, LHC and LC, for shedding light on the structure of a heavy hidden sector.

The SM electroweak gauge interaction of the B -field is unaltered by kinetic mixing to leading order and the procedure of high-precision SM analyses is modified only to second order. Also, the Higgs-portal interactions have been introduced in renormalizable form. As a result, well-explored low-energy physics is not dramatically affected, and changes are just restricted to potentially small corrections.

It turns out that the re-diagonalization of the gauge sector after switching on kinetic mixing is surprisingly straightforward and the results can largely be presented in transparent analytic form. However, the re-diagonalization of the effective mass matrix of the gauge fields, parallel to the re-diagonalization of the mass matrix in the Higgs sector, can in general be carried out analytically only by expanding mass eigenvalues and field eigenvectors in the ratio of SM masses over dark masses, the latter assumed to be large, i.e. in the TeV regime [13].

First we will discuss both Higgs-portal mixing and gauge-kinetic mixing quite generally. Thereafter we will turn to numerical examples for Higgs and vector fields in a hidden sector coupled either by one or two links to the SM, i.e. $1 \oplus 1$ and $1 \oplus 2$ mixing scenarios. Specifically we will address the problem of how to encircle parameters such that the structure of the combined system can be tested. We will analyze the problem of how to extract, at LHC and LC, the basic mass parameters and the mixings between the hidden sector and the measurable SM.

1.1. Higgs Portal : Multiple Couplings

In the extended Higgs sector we will assume that the SM iso-doublet Higgs field ϕ is complemented by a set of n complex scalar fields S_i that generate the hidden gauge boson masses, including the n U(1) gauge bosons $V = \{V_1, \dots, V_n\}$, which are mixed with the hypercharge SM gauge boson. Expanding the fields about the minimum of the scalar potential, the real SM Higgs field H_0 and n hidden-sector Higgs fields $H = \{H_1, \dots, H_n\}$ will emerge, corresponding to scalars located primarily in the visible SM sector and the invisible hidden sector, respectively. The two sectors are coupled weakly and they are linked by bi-linear quartic couplings, leaving the system renormalizable.

Cast into the standard formalism of spontaneous symmetry breaking, the Higgs potential is introduced as

$$\mathcal{V}_{\mathcal{H}} = [\mu_0^2|\phi|^2 + \lambda_0|\phi|^4] + \sum_{i=1}^n [\mu_i^2|S_i|^2 + \lambda_i|S_i|^4] + \sum_{i=1}^n \eta_i|\phi|^2|S_i|^2. \quad (1.1)$$

The μ^2 parameters are negative, shifting the ground states to non-zero vacuum values, and the λ parameters are positive to stabilize the system. As we focus primarily on the direct coupling of the SM Higgs field and the hidden-sector Higgs fields, quartic interactions among the hidden-sector Higgs fields can be ignored to leading order in this context if the couplings of the mixing terms are taken to be small. Their impact on any physical observables will be suppressed when passing the Higgs-portal. [For illustration, the analysis including small quartic mixing in the hidden sector is summarized in Appendix A.

Introducing the vacuum Higgs values v at the minimum of the potential,

$$\phi_0 = (v_0 + H_{0c})/\sqrt{2} \quad \text{and} \quad S_i = (v_i + H_{ic})/\sqrt{2} \quad (1.2)$$

where ϕ_0 is the neutral component of the SM iso-doublet Higgs field ϕ etc, they can be expressed by the potential

parameters after solving the minimum conditions:

$$v_0^2 = [-\mu_0^2 - \frac{1}{2} \sum_{k=1}^n \eta_k v_k^2] / \lambda_0 \rightarrow \frac{-\mu_0^2 / \lambda_0 + \frac{1}{2} \sum \eta_k \mu_k^2 / \lambda_k \lambda_0}{1 - \frac{1}{4} \sum \eta_k^2 / \lambda_k \lambda_0} \quad (1.3)$$

$$v_i^2 = [-\mu_i^2 - \frac{1}{2} \eta_i v_0^2] / \lambda_i \rightarrow \frac{-\mu_i^2 / \lambda_i + \frac{1}{2} \eta_i \mu_0^2 / \lambda_0 \lambda_i - \frac{1}{4} \sum [\eta_i \mu_k^2 - \eta_k \mu_i^2] \eta_k / \lambda_k \lambda_0 \lambda_i}{1 - \frac{1}{4} \sum \eta_k^2 / \lambda_k \lambda_0} \quad \text{for } i = 1, \dots, n. \quad (1.4)$$

Inserting mutually v_0 into v_i and v.v., the set of two equations has been solved for v_0 and v_i supplementing the original values of the individual sectors, $v_0^2 \leftarrow -\mu_0^2 / \lambda_0$ and $v_i^2 \leftarrow -\mu_i^2 / \lambda_i$, before they are coupled by η_i .

The bilinear kinetic terms and the mass terms of the physical Higgs fields are described by the effective Lagrangian:

$$\mathcal{L}_H = \frac{1}{2} \partial \begin{pmatrix} H_0 \\ H \end{pmatrix}_c^T \partial \begin{pmatrix} H_0 \\ H \end{pmatrix}_c - \frac{1}{2} \begin{pmatrix} H_0 \\ H \end{pmatrix}_c^T \mathcal{M}_{Hc}^2 \begin{pmatrix} H_0 \\ H \end{pmatrix}_c \quad \text{with} \quad \mathcal{M}_{Hc}^2 = \begin{pmatrix} M_{0c}^2 & X^T \\ X & M_c^2 \end{pmatrix}. \quad (1.5)$$

The parameter M_{0c}^2 denotes the mass of the SM Higgs boson in the current basis, the matrix M_c^2 denotes the $n \times n$ mass matrix of the Higgs bosons in the hidden sector [for simplicity assumed to be diagonal], and the n -dimensional column vector X accounts for the couplings of the scalars in the SM and the hidden sectors:

$$M_{0c}^2 = 2\lambda_0 v_0^2 \quad (1.6)$$

$$M_c^2 = \text{diag}(2\lambda_1 v_1^2, \dots, 2\lambda_n v_n^2) \quad (1.7)$$

$$X^T = (\eta_1 v_0 v_1, \dots, \eta_n v_0 v_n) \quad (1.8)$$

expressed by the basic parameters of the potential. [In the general case with quartic terms of hidden-sector Higgs fields, the matrix M_c^2 is non-diagonal but symmetric so that it can be diagonalized by an orthogonal transformation. The mixing vector X is changed slightly as a result, see Appendix A.]

The mass matrix in the current [c] representation will be transformed to the diagonal mass matrix in the mass [m] representation by applying the orthogonal transformation \mathcal{O}_H :

$$\mathcal{M}_{Hc}^2 \Rightarrow \mathcal{M}_{Hm}^2 = \mathcal{O}_H \mathcal{M}_{Hc}^2 \mathcal{O}_H^T = \text{diag}(M_{0m}^2, M_m^2) \quad (1.9)$$

while the Higgs fields transform as

$$\begin{pmatrix} H_0 \\ H \end{pmatrix}_c = \mathcal{O}_H^T \begin{pmatrix} H_0 \\ H \end{pmatrix}_m. \quad (1.10)$$

For $n = 2$ and higher, the eigenvalues and eigenfunctions of the mass matrix cannot be written in closed or transparent form anymore. But they can be expanded consistently for small mixing up to second order in the expansion parameter X [13]:

$$M_{0m}^2 = M_{0c}^2 - X^T (M_c^2 - M_{0c}^2)^{-1} X \quad (1.11)$$

$$M_m^2 = M_c^2 + \frac{1}{2} \text{diag} \{ X X^T, (M_c^2 - M_{0c}^2)^{-1} \} \quad (1.12)$$

while the orthogonal transformation matrix up to second order reads

$$\mathcal{O}_H = \begin{pmatrix} 1 - \frac{1}{2} \Omega_H^T \Omega_H & \Omega_H^T \\ -\Omega_H & 1 - \frac{1}{2} \Omega_H \Omega_H^T \end{pmatrix} \quad \text{with} \quad \Omega_H = -(M_c^2 - M_{0c}^2)^{-1} X. \quad (1.13)$$

The corrections of the heavy hidden Higgs masses M_m^2 are in general not diagonal. However, re-diagonalization gives rise to changes of the eigenvalues and mixing matrices only beyond the order considered so that the off-diagonal elements can simply be truncated [see the proof in the Appendix].

By assuming the mass parameters in the hidden sector to be heavy compared with the SM sector and the mixing parameters, the norm of the vector $\|\Omega_H\| \sim \|X\|/\|M^2\|$ is small and serves as an expansion parameter, in parallel with $\|M_0^2\|/\|M^2\|$. The SM Higgs mass parameter $M_{0c}^2 \Rightarrow M_{0m}^2$ however could be modified sizably if the mixing parameter is not much smaller than the SM parameter [consistent with the expansion]. To lowest order, the modifications of the masses and the mixing matrix,

$$M_{0m}^2 \simeq M_{0c}^2 - X^T (M_c^2)^{-1} X \quad (1.14)$$

$$M_m^2 \simeq M_c^2 \quad (1.15)$$

mcc and

$$\mathcal{O}_H \simeq \begin{pmatrix} 1 & \Omega_H^T \\ -\Omega_H & 1 \end{pmatrix} \quad \text{and} \quad \begin{cases} H_{0m} \simeq H_{0c} & + \Omega_H^T H_c \\ H_m \simeq -H_{0c} \Omega_H & + H_c \end{cases} \quad (1.16)$$

are particularly simple. This set of transformations of the wave-functions generates the reduced couplings of the SM-type Higgs boson and the couplings of the hidden Higgs bosons with the SM gauge and matter fields to first order in the mixing.

In the $1 \oplus 1$ Higgs scenario the solution can be reconstructed analytically without any expansion [10, 14]. The mixing matrix is the standard 2×2 matrix built up by $\sin \chi$ and $\cos \chi$ of the rotation angle χ . After reducing the vector Ω_H to the small mixing angle $\Omega_H \simeq \chi$, the above relations are readily recovered from the $(1+n) \times (1+n)$ system, as will be recalled later.

Starting from the lowest order, masses and mixings can iteratively be constructed to arbitrary order in the expansion parameter $\epsilon \sim \|M_0^2\|/\|M^2\|$, $\|X\|/\|M^2\|$, both of which are small for large masses in the hidden sector, compared to SM masses and mixings. The perturbative recursion formulae are derived in the Appendix.

1.2. Kinetic Mixing

The interaction between the SM hypercharge B -field and the set of n gauge $\{V_1, \dots, V_n\}$ fields concentrated in the hidden sector, is described by the Lagrangian

$$\mathcal{L}_V = -\frac{1}{4} \begin{pmatrix} \tilde{W} \\ \tilde{B} \\ \tilde{V} \end{pmatrix}_c^T [1 + \mathcal{S}] \begin{pmatrix} \tilde{W} \\ \tilde{B} \\ \tilde{V} \end{pmatrix}_c + \frac{1}{2} \begin{pmatrix} W \\ B \\ V \end{pmatrix}_c^T \mathcal{M}_{Vc}^2 \begin{pmatrix} W \\ B \\ V \end{pmatrix}_c \quad \text{with} \quad \mathcal{S} = \begin{pmatrix} 0 & 0 & 0 \\ 0 & 0 & s^T \\ 0 & s & 0 \end{pmatrix} \quad (1.17)$$

where \mathcal{M}_{Vc}^2 is the current $(2+n) \times (2+n)$ gauge-boson mass matrix given by

$$\mathcal{M}_{Vc}^2 = M_{Zc}^2 \begin{pmatrix} c_W^2 & -c_W s_W & 0 \\ -c_W s_W & s_W^2 & 0 \\ 0 & 0 & \Delta \end{pmatrix} \quad \text{with} \quad \Delta = M_{Vc}^2 / M_{Zc}^2 \quad (1.18)$$

in terms of the mass parameter $M_{Zc} = \sqrt{g^2 + g'^2} v_0 / 2$, the sine/cosine of the electroweak mixing angle $s_W = \sin \theta_W$ etc, as well as the $n \times n$ dimensionless matrix Δ , after including the mixing of the SM neutral iso-spin W -field and the

hypercharge B -field due to electroweak symmetry breaking. While the field vectors are denoted by $V = \{V_1, \dots, V_n\}$, the field tensors are denoted by $\tilde{V} = \{\tilde{V}_1, \dots, \tilde{V}_n\}$; s is the n -dimensional vector accounting for the kinetic B - V mixings. For the sake of notational simplicity we have refrained from introducing mixing among the fields in the hidden sector, which can easily be added .

Applying an $\text{SL}(2+n, \mathbb{R})$ matrix transformation, consisting of a kinetic transformation [KT] \mathcal{Z} and a rotation, to the gauge fields, the kinetic mixing of the field strengths can be absorbed in the redefinition of the fields. Thereafter, the mass matrix must be diagonalized by a matrix split into the block-diagonalization matrix \mathcal{O}_V and the rotation matrix \mathcal{U}_d re-diagonalizing the mass submatrix in the hidden sector. The block-diagonalization can be performed only approximately; the expansion parameters being $\|s\|$ and $\|M_Z^2/M_V^2\|$, with the norms assumed to be small. The final result of this procedure can be written as follows:

$$\mathcal{L}_V = -\frac{1}{4} \begin{pmatrix} \tilde{A} \\ \tilde{Z} \\ \tilde{V} \end{pmatrix}_m^T 1_N \begin{pmatrix} \tilde{A} \\ \tilde{Z} \\ \tilde{V} \end{pmatrix}_m + \frac{1}{2} \begin{pmatrix} A \\ Z \\ V \end{pmatrix}_m^T \mathcal{M}_{V_m}^2 \begin{pmatrix} A \\ Z \\ V \end{pmatrix}_m \quad \text{with} \quad \begin{pmatrix} W \\ B \\ V \end{pmatrix}_c = \mathcal{Z}^T \mathcal{O}_V^T \mathcal{U}_d^T \begin{pmatrix} A \\ Z \\ V \end{pmatrix}_m \quad (1.19)$$

leading to the massless photon field A_m , and the massive vector fields Z_m and V_m . The KT matrix and the block- and re-diagonalization matrices read

$$\mathcal{Z} = \begin{pmatrix} s_W & c_W & 0 \\ c_W & -s_W & 0 \\ 0 & -\sigma s & \sigma \end{pmatrix}, \quad \mathcal{O}_V \simeq \begin{pmatrix} 1 & 0 & 0 \\ 0 & 1 & \Omega_V^T \\ 0 & -\Omega_V & 1 \end{pmatrix} \quad \text{and} \quad \mathcal{U}_d = \begin{pmatrix} 1 & 0 & 0 \\ 0 & 1 & 0 \\ 0 & 0 & U_d \end{pmatrix} \quad (1.20)$$

with the n -dimensional column vector Ω_V

$$\Omega_V \simeq -s_W (M_{Z_c}^2/M_{V_c}^2) s \quad (1.21)$$

to lowest order in the mixing. [\mathcal{U}_d actually proves ineffective to lowest order, as derived in the Appendix.]

The submatrix σ in \mathcal{Z} is a symmetric $n \times n$ matrix defined by the dyadic product ss^T of the mixing parameters s ,

$$\sigma = (1 - ss^T)^{-\frac{1}{2}} = u^T \sigma_d u \quad (1.22)$$

which can be diagonalized by the $n \times n$ orthogonal matrix u , generating the diagonal matrix σ_d . The set of eigenvalues of the dyadic matrix ss^T consists of one non-zero value $\|s\|^2$ followed by $n-1$ zero values, giving rise to the $n \times n$ diagonal matrix $\sigma_d = \text{diag}[(1 - \|s\|^2)^{-\frac{1}{2}}, 1, \dots, 1]$. The spectrum and the eigenvectors are derived in the Appendix.

Switching from the current [c] basis to the mass [m] basis, the mass matrix is transformed, up to second order, to the diagonal $(2+n) \times (2+n)$ mass matrix $\mathcal{M}_{V_m}^2$ in Eq. (1.19), representing the zero photon mass and the non-zero mass eigenvalues up to second order as

$$M_\gamma^2 = 0 \quad (1.23)$$

$$M_{Z_m}^2 \simeq M_{Z_c}^2 - s_W^2 s^T (M_{B_c}^4/M_{V_c}^2) s \rightarrow M_{Z_c}^2 \quad (1.24)$$

$$M_{V_m}^2 \simeq U_d M_{V_c}^2 U_d^T + \frac{1}{2} \text{diag}\{ss^T, M_{V_c}^2\} \quad (1.25)$$

where U_d diagonalizes the matrix $M_{V_c}^2$ up to the second-order approximation of the mixing.

Special attention should be payed to the peripheral null-vector in the matrix \mathcal{Z} . This form is essential to keep the SM gauge interactions intact to leading order. This is apparent by noting the covariant derivative which transform as

$$\begin{aligned} iD &= i\partial - gT_3 W_c - g'Y B_c - g_V Y_V^T V_c \\ &\simeq i\partial - eQA_m - g_Z(T_3 - Y)Z_m - (g_V Y_V^T - g'Y s^T) V_m \end{aligned} \quad (1.26)$$

with $Y_V = \{Y_{V1}, \dots, Y_{Vn}\}$ and up to linear approximation in the kinetic mixing; as usual, $e = gs_W$, $Q = T_3 + Y$ and $g_Z = [g^2 + g'^2]^{1/2}$. The coefficients of the A and Z fields are not altered preserving the standard structures in the original electroweak sector after electroweak symmetry breaking at this level.

2. $1 \oplus 1$ ANALYSIS

The simplest example of portal models combines the SM with just one new degree of freedom in the hidden sector. With some elements worked out already a while ago, cf. Ref. [3], we extend the analysis in this section at the level of phenomenology as well as analytical solutions based on perturbative expansions. Note that the Higgs and the gauge sectors are entangled, the connecting link being the transformed vacuum expectation values of the Higgs fields affecting the current mass parameters of the gauge fields.

2.1. Higgs system

Specifying the notation in the previous sections, the physical Higgs masses $M_{0m/1m}$ and the Higgs mixing angle χ , derived from the current Higgs mass matrix,

$$\mathcal{M}_H^2 = \begin{pmatrix} 2\lambda_0 v_0^2 & \eta_1 v_0 v_1 \\ \eta_1 v_0 v_1 & 2\lambda_1 v_1^2 \end{pmatrix} \quad (2.1)$$

are given by

$$M_{0m}^2 = \lambda_0 v_0^2 + \lambda_1 v_1^2 - \sqrt{(\lambda_1 v_1^2 - \lambda_0 v_0^2)^2 + (\eta_1 v_0 v_1)^2} \simeq 2\lambda_0 v_0^2 - \eta_1^2 v_0^2 / 2\lambda_1 \quad (2.2)$$

$$M_{1m}^2 = \lambda_0 v_0^2 + \lambda_1 v_1^2 + \sqrt{(\lambda_1 v_1^2 - \lambda_0 v_0^2)^2 + (\eta_1 v_0 v_1)^2} \simeq 2\lambda_1 v_1^2 + \eta_1^2 v_0^2 / 2\lambda_1 \quad (2.3)$$

$$\tan 2\chi = -\eta_1 v_0 v_1 / (\lambda_1 v_1^2 - \lambda_0 v_0^2) \simeq -\eta_1 v_0 / \lambda_1 v_1 \quad (2.4)$$

up to the second order approximation in η for the masses. It should be noted that the leading mass corrections are not suppressed by the large hidden scale v_1 , in contrast to the mixing angle. The current Higgs fields $\{H_{0c}, H_{1c}\}$ and the mass Higgs fields $\{H_{0m}, H_{1m}\}$ are related by the orthogonal transformation \mathcal{O}_H^T :

$$\begin{pmatrix} H_0 \\ H_1 \end{pmatrix}_c = \begin{pmatrix} \cos \chi & -\sin \chi \\ \sin \chi & \cos \chi \end{pmatrix} \begin{pmatrix} H_0 \\ H_1 \end{pmatrix}_m \quad (2.5)$$

where $\cos \chi$ can be assumed non-negative without loss of generality. These three observables can be exploited, in return, to extract the individual vacuum parameters $\lambda_0 v_0^2$, $\lambda_1 v_1^2$ and $\eta_1 v_0 v_1$ according to

$$2\lambda_0 v_0^2 = M_{0m}^2 \cos^2 \chi + M_{1m}^2 \sin^2 \chi \quad (2.6)$$

$$2\lambda_1 v_1^2 = M_{0m}^2 \sin^2 \chi + M_{1m}^2 \cos^2 \chi \quad (2.7)$$

$$2\eta_1 v_0 v_1 = -(M_{1m}^2 - M_{0m}^2) \sin 2\chi. \quad (2.8)$$

While the measurement of the two Higgs masses, M_{0m} and M_{1m} , is self-evident, the mixing parameter $\cos \chi$ can be determined from the Higgs-gauge boson vertex, i.e.

$$g[H_{0m}WW] = 2M_{0m}^2 \cos \chi / v_0 \quad (2.9)$$

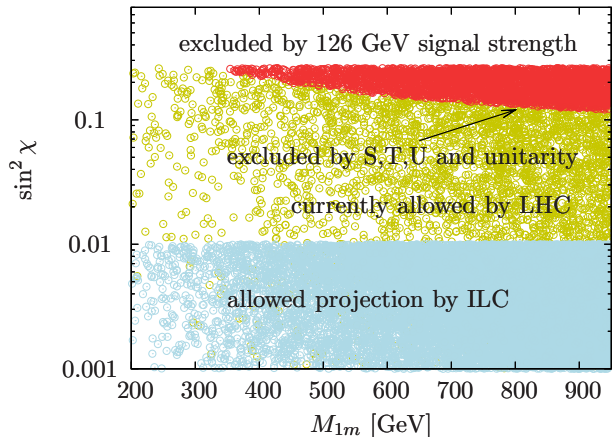


FIG. 1: Scan over the parameter points of the $1 \oplus 1$ including current H_{0m} measurements and exclusion limits for H_{1m} . Kinetic mixing is switched off for transparency of the result; invisible Higgs widths are included in the scan. Also included are constraints from unitarity and oblique corrections [15]. We show projections of the M_{1m} and $\sin^2 \chi$ region that is currently allowed by the LHC (yellow) and the parameter region where there will be no constraint from a combined ILC+LHC measurement.

where v_0 is given by the W mass

$$M_W = g v_0 / 2 \quad (2.10)$$

with the $SU(2)_L$ gauge coupling g derived from the measured W -width in a model-independent way to leading order. [The hypercharge coupling g' is derived correspondingly from combining the electron electromagnetic-magnetic coupling $e = g s_W$ and with the hypercharge relation $g' = e / c_W$.]

The quartic couplings λ_0, λ_1 , or equivalently the vacuum expectation values v_0, v_1 , can be separated only by measuring the triple Higgs couplings. Denoting the current triple $H_{ic} H_{jc} H_{kc}$ Higgs couplings by t_{ijk}^c [$i, j, k = 0, 1$], they can be expressed by the physical $H_{pm} H_{qm} H_{rm}$ couplings t_{pqr}^m [$p, q, r = 0, 1$] in the mass basis as

$$t^c = \mathcal{O}_H^T \otimes \mathcal{O}_H^T \otimes \mathcal{O}_H^T t^m. \quad (2.11)$$

The tensor components can be written as

$$t_{000}^m = \frac{1}{2} M_{0m}^2 (c_\chi^3 / v_0 + s_\chi^3 / v_1) \quad (2.12)$$

$$t_{001}^m = -\frac{1}{6} (2M_{0m}^2 + M_{1m}^2) (c_\chi / v_0 - s_\chi / v_1) c_\chi s_\chi \quad (2.13)$$

$$t_{011}^m = \frac{1}{6} (M_{0m}^2 + 2M_{1m}^2) (s_\chi / v_0 + c_\chi / v_1) c_\chi s_\chi \quad (2.14)$$

$$t_{111}^m = -\frac{1}{2} M_{1m}^2 (s_\chi^3 / v_0 - c_\chi^3 / v_1) \quad (2.15)$$

with the abbreviations $c_\chi = \cos \chi$ etc; they are symmetric under index permutations. The Feynman rules follow from multiplying the above equations by a minus sign and a combinatorial factor that counts the number of the identical external legs. The parameter v_1 of the hidden sector is naturally associated either with [small] mixing coefficients or with coupling/mass suppressed H_1 degrees of freedom.

For illustration purposes, we pick, with $M_{0m} = 125$ GeV, a representative parameter point

$$\cos^2 \chi = 0.9, \quad M_{1m} / M_{0m} = 2.5, \quad v_1 / v_0 = 2 \quad (2.16)$$

from the scan of the allowed points depicted in Fig. 1 [choosing a SM-like width of H_{0m}]. Identifying the mass of H_{0m} with 125 GeV, the global area of the two unknown parameters, i.e. the second Higgs mass M_{1m} and the mixing $\sin^2 \chi$, is tightly constrained by future precision measurements of the H_{0m} boson. For a numerical investigation of the above parameter point we adopt the extrapolations to 3 ab^{-1} for LHC at 14 TeV and adopt an energy of 250 GeV for ILC as provided in Ref. [16]. A measurement of $\cos^2 \chi$ and the masses M_{1m} and M_{0m} , which will be well established at the quoted LHC luminosity, is not enough to separate vacuum expectation values from quartic couplings in the most general and complete analysis of the $1 \oplus 1$ system. We need (at least) one additional measurement in order to

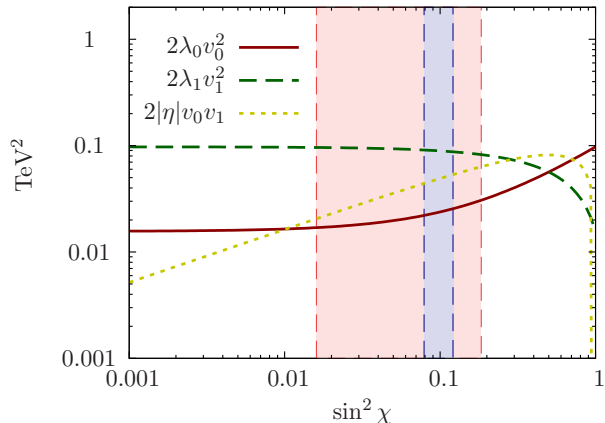


FIG. 2: The system of mass relations in Eqs. (2.6), (2.7) and (2.8) for the parameter point in Eq. (2.16). The light red band gives the expected 1σ interval for an LHC measurement of H_{0m} at the luminosity of 3 ab^{-1} . The blue band corresponds to the parameter range allowed by an ILC measurement at $\sqrt{s} = 250 \text{ GeV}$ with the same luminosity of 3 ab^{-1} .

reconstruct all the parameters individually.

There are two independent approaches to this problem, depending on the size of the invisible Higgs branching ratios. For large values, we can use an invisible Higgs measurement to constrain the parameter $\sin^2 \chi$ as described in Ref. [10].

Since recent measurements of H_{0m} point towards a SM-like total width (at least when $SU(2)_L$ doublets are involved [17]) we investigate a different possibility in the following, assuming no direct partial decay width of H_{0m} to the hidden sector. Then phenomenology is dominated by mixing only and we can use an experimentally measured region of $\sin^2 \chi$ to constrain the system of mass relations in Eqs. (2.6), (2.7) and (2.8) as shown in Fig. 2. The additional information to reconstruct the individual parameters should then be made available from the measurement of the trilinear Higgs couplings in Eqs. (2.12)-(2.15) [10, 18], which can be phenomenologically accessed via light diHiggs production, i.e. predominantly $gg \rightarrow H_{0m}H_{0m}$ at the LHC [19]. [Recall that in $1 \oplus n$ scenarios v_0 is known from the W mass and the $SU(2)_L$ gauge coupling g measured by the W width, both of which are not affected by $U(1)$ mixings.]

Recent analyses [20] indicate that a variation of the trilinear Higgs coupling is only feasible in the context of the SM in the $b\bar{b}\tau^+\tau^-$ channel [21] if possible at all. Rare Higgs decays such as $H_{0m}H_{0m} \rightarrow b\bar{b}\gamma\gamma$ [22] are clean [$S/B = 0.7$ for 12 signal events in 3 ab^{-1} [20].] Nevertheless the involved uncertainties are too large and the signal yield is too small to obtain a more fine grained picture. In contrast to the SM, however, the $1 \oplus 1$ scenario offers the possibility to discriminate the $H_{1m} \rightarrow H_{0m}H_{0m}$ signal region from the “continuum” $H_{0m}H_{0m}$ production. Upon correlating the two regions we can constrain v_1 in different channels: Electroweak precision measurements, even for rather small mixing angles $\sin^2 \chi \sim 0.1$, indicate that the mass splitting between the 125 GeV boson and H_{1m} must not be too large. Observing a cascade decay $H_{1m} \rightarrow H_{0m}H_{0m}$ therefore implies small boosts of the H_{0m} bosons and the analysis of the $H_{0m}H_{0m} \rightarrow b\bar{b}\tau^+\tau^-$ final state is not applicable anymore. On the other hand, $H_{0m}H_{0m} \rightarrow b\bar{b}\gamma\gamma$ is inclusive in this sense and we can extract a limit on v_1 in this channel when selecting invariant masses $m(H_{0m}H_{0m}) \sim m(H_{1m})$. The complimentary phase space region can again be tackled in the boosted selection using the methods of Ref. [21].

In both analyses interference plays an important role. We therefore use a complete leading order calculation keeping the full top mass dependence following Ref. [18]. The result for the two signal regions including the expected measured 1σ interval at 14 TeV and 3 ab^{-1} is shown in Figs. 3a and 3b. The dip structure of Fig. 3b highlights the importance of the interference effects: for $v_1 \sim v_0/\tan \chi \sim 80 \text{ GeV}$ the resonant production has a global minimum due to the vanishing of t_{011}^m . For values $v_1 < v_0/\tan \chi$ the $gg \rightarrow H_{1m} \rightarrow H_{0m}H_{0m}$ diagrams interfere destructively with the $gg \rightarrow H_{0m}H_{0m}$ box contributions, but the t_{001}^m grows quickly to outrun the suppression. For the away-from-resonance region this interference is always destructive, i.e. the smaller v_1 the larger t_{000}^m and the smaller the resulting $pp \rightarrow H_{0m}H_{0m}$ cross section until the trilinear coupling t_{001}^m compensates the

enhanced destructive interference of t_{000}^m with the box contribution and the propagator suppression for very small values of v_1 . In this sense H_{1m} “leaks” into the H_{0m} measurement region and must not be discarded in the actual analysis.

The region of large v_1 values is determined by the $\cos^2 \chi$ pieces of t_{000}^m and t_{001}^m and the asymptotic cross section settles at a smaller cross section with respect to the SM, mostly as a consequence of the $\cos^4 \chi$ suppression. By contrast, given the small mixing and the kinematic suppression, it is impossible to observe t_{011}^m and t_{111}^m at the LHC [18].

Depending on the scenario, systematics etc., either the peak or the continuum analysis can perform better. In any case, both analyses can be used for cross checks and for lifting the degeneracy, if present, of the peak analysis. Using the currently known results we find a lower limit of

$$v_1 > 200 \text{ GeV} \quad (2.17)$$

with the $b\bar{b}\tau^+\tau^-$ analysis to be compared with the slightly larger bound for the chosen parameter point. This interval can be mapped onto the allowed region of Fig.2 constraining $\eta, \lambda_1, \lambda_0$. However, as can be seen from Figs.3a and 3b, the model-independent separation of the λ parameters and the vacuum expectation value v_1 is in general not feasible for the planned luminosities at LHC as an upper bound on v_1 is very loose if it can be established at all. Even at an e^+e^- collider running at $\sqrt{s} = 500$ GeV (Fig.4) we can only extract a lower limit on v_1 at an integrated luminosity of 2 ab^{-1} [see Ref. [23] for a general discussion of measuring the trilinear Higgs coupling at a linear collider]. However, given that at this luminosity the uncertainties are still statistics-driven, there might be the possibility to extract an upper limit on v_1 in the far future. In fact, the quoted uncertainty band is entirely dominated by the statistical uncertainty of the signal counts as the search is essentially background-free [24].

However, in theoretical scenarios which predict the values of the gauge coupling and the hypercharge in the hidden sector, the vacuum expectation value v_1 can be determined from the two vector-boson masses:

$$v_1/v_0 = [g/2]/[g_V Y_V] \times M_{Vc}/M_W. \quad (2.18)$$

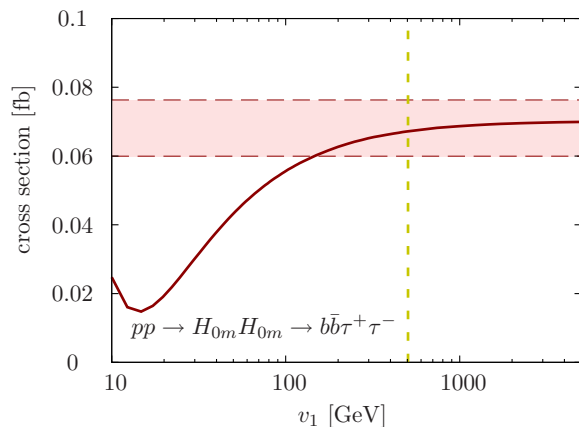


FIG. 3a: Dihiggs production cross section for the parameter point in Eq. (2.16) as function of v_1 *excluding* the $H_{1m} \rightarrow H_{0m}H_{0m}$ signal region by cutting out the H_{1m} resonance via an invariant mass cut on the diHiggs system $m(H_{0m}H_{0m})$. We use the efficiencies of Ref. [21]. The vertical line represents the benchmark value of v_1 that can be extracted from the vector-boson masses in concrete models.

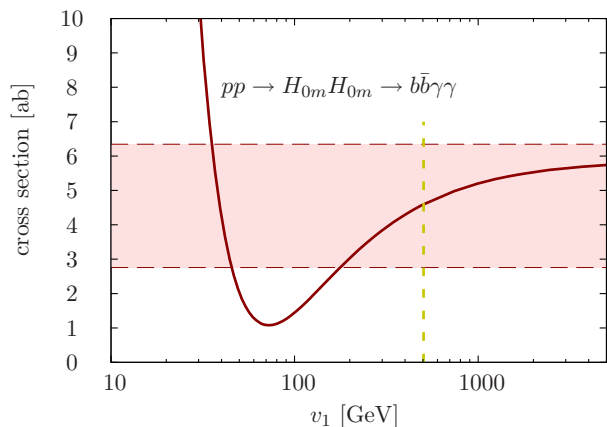


FIG. 3b: Dihiggs production cross section for Eq. (2.16) as function of v_1 *selecting* the $H_{1m} \rightarrow H_{0m}H_{0m}$ signal region by cutting out the H_{1m} resonance via an invariant mass cut on the diHiggs system $m(H_{0m}H_{0m})$. We use the efficiencies of Ref. [20]. The vertical line represents the benchmark value of v_1 that can be extracted from the vector-boson masses in concrete models.

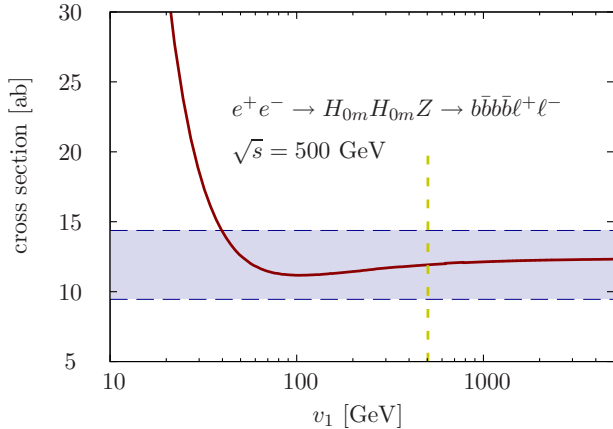


FIG. 4: Double Higgs-strahlung at a 500 GeV e^+e^- collider as a function of v_1 for the chosen parameter point. The blue band corresponds to the parameter range allowed by a measurement with a 2 ab^{-1} sample. We adopt efficiencies from Ref. [24].

Thus, the fundamental current parameters $\lambda_0, \mu_0^2; \lambda_1, \mu_1^2; \eta$ in the Higgs potential can, in principle, be extracted from experimental data, the combinations $\lambda_0 v_0^2; \lambda_1 v_1^2; \eta_1 v_0 v_1$ easily extracted from masses and mixings, and the v 's separately bounded from trilinear Higgs couplings or derived from vector-mass measurements in specified theories. When the gauge couplings and charges are predicted theoretically, all the fundamental Higgs parameters can be extracted.

2.2. Kinetic Mixing

Analogously, the mixing of the gauge sector can be worked out explicitly. The kinetic term and the mass term are diagonalized by a $\text{SL}(3, \text{R})$ kinetic transformation and an orthogonal 3×3 rotation matrix \mathcal{O}_V as

$$\begin{pmatrix} W \\ B \\ V \end{pmatrix}_c = \begin{pmatrix} s_W & c_W & 0 \\ c_W & -s_W & -s\sigma \\ 0 & 0 & \sigma \end{pmatrix} \begin{pmatrix} 1 & 0 & 0 \\ 0 & \cos\theta & -\sin\theta \\ 0 & \sin\theta & \cos\theta \end{pmatrix} \begin{pmatrix} A \\ Z \\ V \end{pmatrix}_m \quad (2.19)$$

with $\sigma = 1/\sqrt{1-s^2}$. The masses, in the current basis,

$$M_{W_c}^2 = g^2 T_3^2 v_0^2 = g^2 v_0^2/4 \quad (2.20)$$

$$M_{B_c}^2 = g'^2 Y_0^2 v_0^2 = g'^2 v_0^2/4 \quad (2.21)$$

$$M_{Z_c}^2 = [g^2 + g'^2] v_0^2/4 \quad (2.22)$$

$$M_{V_c}^2 = g_V^2 Y_V^2 v_1^2 \quad (2.23)$$

are defined by the gauge couplings, the vacuum expectation values, and the $\text{SU}(2)$ T_3 and the $\text{U}(1)$ Y charges of the Higgs fields. Since the charged W -field does not mix with the vector field in the hidden sector, the measured values of the W -mass and width determine the parameters g and v_0 and the SM relations $g = e/s_W$ and $g' = e/c_W$ define s_W , g' , $g_Z = [g^2 + g'^2]^{1/2}$ and M_{Z_c} before mixing. The [neutral] current masses are transformed to the vanishing photon mass $M_{A_m} = 0$ and two physical non-zero gauge boson masses M_{Z_m}, M_{V_m} by the rotation angle θ . The exact and the approximate forms, expanded up to second order in s and $\|M_{Z_c}^2/M_{V_c}^2\|$, may be denoted as

$$M_{Z_m}^2 = M_{Z_c}^2 \left\{ (1 + s_W^2 \sigma^2 s^2 + \sigma^2 \Delta) - \sqrt{(1 + s_W^2 \sigma^2 s^2 + \sigma^2 \Delta)^2 - 4\sigma^2 \Delta} \right\} / 2 \simeq M_{Z_c}^2 + \dots \quad (2.24)$$

$$M_{V_m}^2 = M_{Z_c}^2 \left\{ (1 + s_W^2 \sigma^2 s^2 + \sigma^2 \Delta) + \sqrt{(1 + s_W^2 \sigma^2 s^2 + \sigma^2 \Delta)^2 - 4\sigma^2 \Delta} \right\} / 2 \simeq M_{V_c}^2 + s^2 M_{V_c}^2 + \dots \quad (2.25)$$

$$\tan 2\theta = 2s_W \sigma s / (1 - s_W^2 \sigma^2 s^2 - \sigma^2 \Delta) \simeq -2s_W (M_{Z_c}^2/M_{V_c}^2) s + \dots \quad (2.26)$$

vertex	type	exact	expansion in mixing
3-gauge bosons	$A_m WW$	e	e
	$Z_m WW$	$g_Z c_W^2 c_\theta$	$g_Z c_W^2$
	$V_m WW$	$-g_Z c_W^2 s_\theta$	$g_Z c_W^2 s_W s M_{Z_c}^2 / M_{V_c}^2$
gauge boson - fermion	$A_m ff$	$e Q_f$	$e Q_f$
	$Z_m ff$	$g_Z (T_3^f - s_W^2 Q_f) c_\theta - g' Y_f \sigma s s_\theta$	$g_Z (T_3^f - s_W^2 Q_f)$
	$V_m ff$	$-g_Z (T_3^f - s_W^2 Q_f) s_\theta - g' Y_f \sigma s c_\theta$	$-g' Y_f s$ $+g_Z (T_3^f - s_W^2 Q_f) s_W s M_{Z_c}^2 / M_{V_c}^2$
Higgs - gauge boson	$H_{0m} WW$	$2M_{W_c}^2 c_\chi / v_0$	$2M_{W_c}^2 [1 - \frac{1}{4}(\eta_1 v_0 / \lambda_1 v_1)^2] / v_0$
	$H_{1m} WW$	$-2M_{W_c}^2 s_\chi / v_0$	$M_{W_c}^2 (\eta_1 / \lambda_1) / v_1$
	$H_{0m} Z_m Z_m$	$2M_{Z_c}^2 [(c_\theta + s_W \sigma s s_\theta)^2 (c_\chi / v_0) + \sigma^2 \Delta s_\theta^2 (s_\chi / v_1)]$	$2M_{Z_c}^2 [1 - \frac{1}{4}(\eta_1 v_0 / \lambda_1 v_1)^2] / v_0$
	$H_{1m} Z_m Z_m$	$2M_{Z_c}^2 [(c_\theta + s_W \sigma s s_\theta)^2 (-s_\chi / v_0) + \sigma^2 \Delta s_\theta^2 (c_\chi / v_1)]$	$M_{Z_c}^2 (\eta_1 / \lambda_1) / v_1$
	$H_{0m} Z_m V_m$	$2M_{Z_c}^2 [(c_\theta + s_W \sigma s s_\theta)(-s_\theta + s_W \sigma s c_\theta)(c_\chi / v_0) + \sigma^2 \Delta c_\theta s_\theta (s_\chi / v_1)]$	$2M_{Z_c}^2 s_W s [1 - M_{Z_c}^2 / M_{V_c}^2] / v_0$
	$H_{1m} Z_m V_m$	$2M_{Z_c}^2 [(c_\theta + s_W \sigma s s_\theta)(-s_\theta + s_W \sigma s c_\theta)(-s_\chi / v_0) + \sigma^2 \Delta c_\theta s_\theta (c_\chi / v_1)]$	$M_{Z_c}^2 s_W [2 + \eta_1 / \lambda_1] s / v_1$

TABLE I: 3-vertices of gauge bosons, fermions and Higgs bosons. The vertices are expanded up to non-vanishing first/second order in the kinetic and Higgs mixings. [Standard tensor and fermion bases are not noted explicitly.]

with $\Delta = M_{V_c}^2 / M_{Z_c}^2$.

The vertices relevant for measuring the parameters of the theory, are collected in Tab. I.

The direct measurement of the W, Z_m, V_m mass parameters [see e.g. Refs. [25, 26] for V_m searches as performed by ATLAS and CMS] in the mass basis together with the indirect determination of the mass parameters in the current basis in Eqs. (2.24), (2.25) and (2.26) allows for a complete analysis of the fundamental vector parameters, including

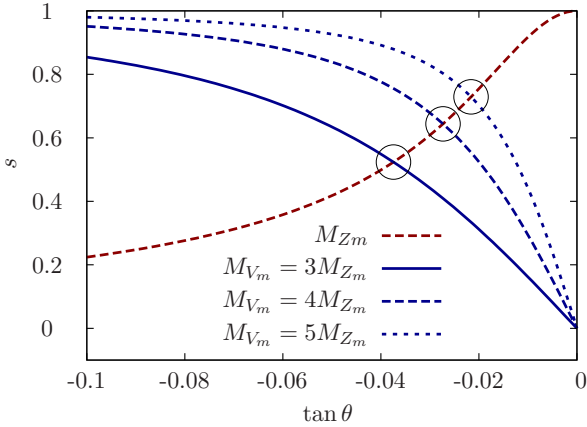


FIG. 5a: Extraction of the kinetic mixing parameters s and $\tan \theta$ from a sample of measured values M_{Z_m} and M_{V_m} from Eqs. (2.27) and (2.28).

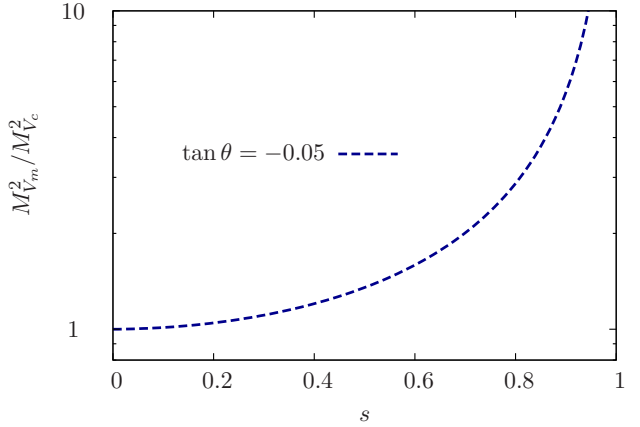


FIG. 5b: Shift of the mass M_{V_m} from M_{V_c} in the hidden sector, depending on the kinetic mixing parameter s for a representative rotation parameter $\tan \theta$, from Eq. (2.29).

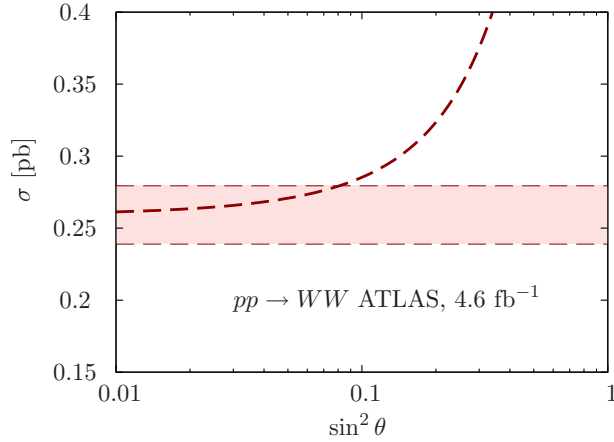


FIG. 6: $pp \rightarrow WW$ cross section as reported in Ref. [28] and the cross section as a function of $\sin^2 \theta$ for s neglected after removing the V_m resonance contribution.

the KT parameter s and the rotation angle θ . From the two relations

$$M_{Z_m}^2/M_{Z_c}^2 = 1 + s_W \frac{s}{\sqrt{1-s^2}} \tan \theta \quad (2.27)$$

$$M_{V_m}^2/M_{Z_c}^2 = 1 - s_W \frac{s}{\sqrt{1-s^2}} \cot \theta \quad (2.28)$$

the mixing parameters, s and $\tan \theta$ can be extracted, Fig. 5a. [Note that due to pure U(1) mixing the weak couplings and v_0 are fixed and measurable quantities, as outlined above, and M_{Z_c} is known.] These values can be exploited to derive the third mass parameter M_{V_c} in the current basis:

$$\begin{aligned} M_{V_c}^2/M_{V_m}^2 &= (1-s^2) M_{Z_m}^2/M_{Z_c}^2 \\ &= 1 - s^2 + s_W s \sqrt{1-s^2} \tan \theta \end{aligned} \quad (2.29)$$

cf. Fig. 5b. These results can be cross-checked for internal consistency by experimentally analyzing vertices collected in Tab. I. Note that oblique corrections due to kinetic mixing are typically less important as compared to Higgs mixing since they scale $\sim s^2 M_{Z_m}^2/M_{V_m}^2$ [27]. Explicit calculation proves that they lead to bounds which are comparable to the limits currently set by ATLAS and CMS (see below).

Current constraints on anomalous triple gauge boson vertices, obtained by ATLAS [28] and CMS [29], restrict $\sin^2 \theta$ to $\lesssim 0.1$, Fig. 6, which becomes comparable to the LEP combination [30]. The WW analysis is highly sensitive to modifications denoted in Tab. I, in light of a tree-level radiation zero in the SM [31]. There exists a completely destructive interference between the W radiation diagrams and the Feynman graph involving the ZWW vertex in the SM. Any (non-global) deviation from the SM-predicted coupling pattern destroys this characteristic angular dip structure resulting in an increase of the total cross section.² Therefore, the integrated cross section [supplemented by a jet veto in the actual analysis] is very sensitive to the suppression of the $Z_m WW$ coupling, which can be used to extract an upper limit on $\sin^2 \theta$ even if the V_m is too heavy to be measured directly.

Note that the $H_{0m} WW$ coupling is not affected by gauge-kinetic mixing so that it can be used to measure $\cos \chi$ individually.

Subsequently, the measurement of the $H_{0m} Z_m Z_m$ vertex can in principle be used to measure the allowed range of the shift of Tab. I. Some concrete models of U(1) mixing in the field and string theories [4, 9] predict the mixing

² This is strictly true at tree level. Gluon induced channels of the higher order-corrected cross section lift the radiation zero.

parameter to be $\lesssim 10^{-3}$, but string models in general allow for rather large s values well in the sensitivity range of LHC (and ILC). A hierarchy $s \ll \eta$ then results in modification of the H_{0m} couplings dominated by the Higgs mixing. This leaves Drell-Yan-like production of V_m as probably the best search strategy in the mass region that can be covered by the LHC and future colliders, Fig. 7. Once the vector-boson mass range is known from LHC, LC scans can improve the sensitivity to measurements of the kinetic mixing parameter s .

3. $1 \oplus 2$ ANALYSIS

To exemplify the analytic and numerical analyses of the preceding sections further, we shall discuss next a more complicated system where the SM Higgs sector is connected by portal interactions with two Higgs systems in the hidden sector, and the U(1) hypercharge field B is mixed kinematically with two abelian U(1) fields $V_{1,2}$ in the hidden sector with charges $Y_{V_{1,2}}$. Such a system may be generated quite easily in superstring theories.

The microscopic parameters in the Higgs sector are chosen such that physical masses are centered around 125, 300, 1000 GeV before mixing. For illustration purposes we take these mass parameters to derive v_1, v_2 for quartic Higgs-coupling values $\lambda_0 = \lambda_1 = \lambda_2$ and set $\eta_2 = \eta_1/2$, such that $\eta = \eta_1$ is the only free parameter left. The B mass associated with the Standard Model is fixed at $M_B = \frac{1}{4}g'^2v_0^2$, the gauge masses in the hidden sector are chosen as 300 and 1000 GeV. The kinetic mixing vector in the gauge sector, defined as $s = |s|[\cos \phi, \sin \phi]$, is varied by running $|s|$ from 0 to 1, with $\sin \phi = 1/\sqrt{2}$ kept fixed. This choice of free parameters is chosen minimal for the sake of transparency.

3.1. Higgs system

Reading off the bilinear mass terms from the Higgs-portal Lagrangian, the Higgs mass matrix turns out to be

$$\mathcal{M}_{Hc}^2 = \begin{pmatrix} 2\lambda_0 v_0^2 & \eta_1 v_0 v_1 & \eta_2 v_0 v_2 \\ \eta_1 v_0 v_1 & 2\lambda_1 v_1^2 & 0 \\ \eta_2 v_0 v_2 & 0 & 2\lambda_2 v_2^2 \end{pmatrix} \Rightarrow \begin{pmatrix} M_{0c}^2 & X^T \\ X & M_c^2 \end{pmatrix}. \quad (3.1)$$

This 3×3 matrix could in principle be diagonalized analytically, but the result is not transparent anymore. In the case of small mixing the approximate results of the previous section can be applied. In general, however, numerical

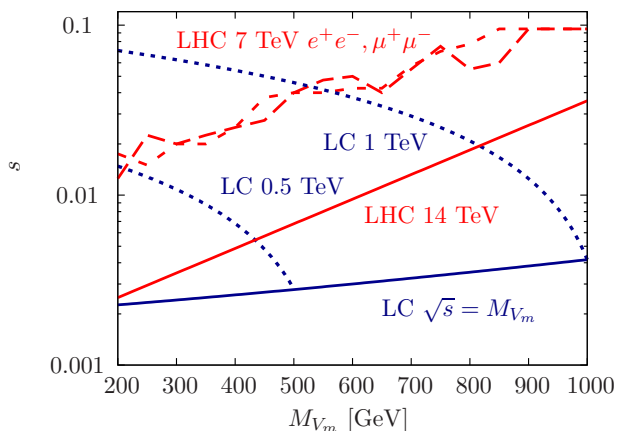


FIG. 7: 95% exclusion limits in the $[M_{V_m}, s]$ plane for the 7 TeV ATLAS V_m analysis (for $V_m \rightarrow \mu^+\mu^-$ and $V_m \rightarrow e^+e^-$ [25, 26, 32]) and a projection based on the extrapolation of these results to 14 TeV and 300 fb^{-1} . The LC limit corresponds to $e^+e^- \rightarrow \text{visible}$ excluding top quarks and Bhabha scattering. We have chosen center-of-mass energies of 500 GeV and 1 TeV (dotted curves) with a bremsstrahlung spectrum modelled as reported in Ref. [33]; the full line predicts the maximum sensitivity to the mixing parameter s for a scan at the c.m. energy $\sqrt{s} \simeq M_{V_m}$. Note, that these exclusion limits are sensitive to the dynamics in the hidden sector via the V_m branching ratio; we only take partial decay widths to SM matter into account in this plot.

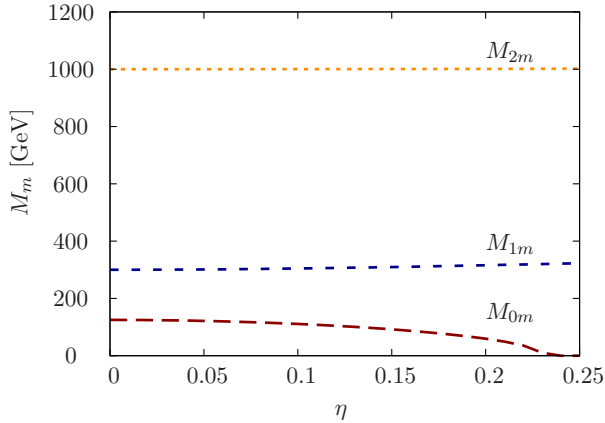


FIG. 7a: Eigenvalues of the matrix Eq. (3.1) as a function of the Higgs mixing. The choice of parameters before mixing is described in the text.

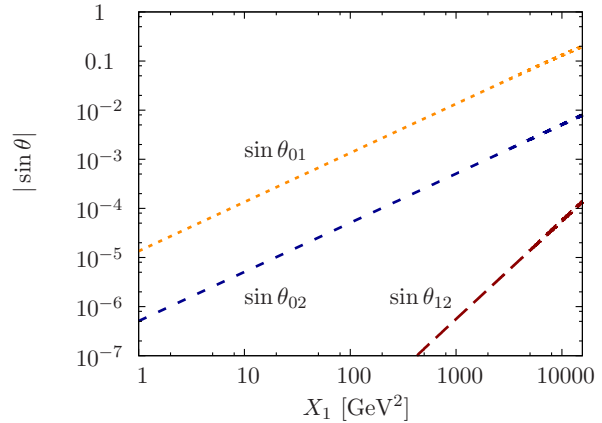


FIG. 7b: Sines of the rotation angles that diagonalize the mass matrix in Eq. (3.1) via the orthogonal matrix $\mathcal{O}_H = R_2(\theta_{01})R_1^T(\theta_{02})R_0(\theta_{12})$. The parameter choices are described in the text and are identical with Fig. 7a.

methods will be adopted and the results will be illustrated in figures.

The three eigenvalues of the mass matrix \mathcal{M}_{Hc}^2 are displayed in Fig. 7a for the fixed parameters as defined earlier, but the mixing parameter η parameterizing the value of X is varied. For small mixing, and large scales of the hidden sector, the masses are given analytically by

$$M_{0m}^2 = 2\lambda_0 v_0^2 - \eta_1^2 v_0^2 / 2\lambda_1 - \eta_2^2 v_0^2 / 2\lambda_2 \quad (3.2)$$

$$M_{1m}^2 = 2\lambda_1 v_1^2 + \eta_1^2 v_0^2 / 2\lambda_1 \quad (3.3)$$

$$M_{2m}^2 = 2\lambda_2 v_2^2 + \eta_2^2 v_0^2 / 2\lambda_2 \quad (3.4)$$

in second order approximation of the mixing.

The orthogonal matrix \mathcal{O}_H in Eq. (1.10) is most elegantly parameterized by the three rotation angles $\theta_{01}, \theta_{02}, \theta_{12}$ associated with the rotations of the 01, 02, 12 planes, i.e. $\mathcal{O}_H = R_2(\theta_{01})R_1^T(\theta_{02})R_0(\theta_{12})$. The sine-functions of the angles are shown in Fig. 7b for varied mixings X as defined above. For small mixing the sines of the rotation angles read

$$\sin \theta_{01} \simeq -\eta_1 v_0 / 2\lambda_1 v_2 \quad (3.5)$$

$$\sin \theta_{02} \simeq -\eta_2 v_0 / 2\lambda_2 v_2 \quad (3.6)$$

$$\sin \theta_{12} \simeq 0 \quad (3.7)$$

up to linear order in the mixing.

Given the parameters, masses and mixings, of the physical states, the production cross sections and the decay branching ratios can be predicted in the standard way.

The mixing modifies the couplings of the original SM Higgs boson to the W -gauge bosons and it generates the corresponding couplings to the original Higgs bosons in the hidden sector:

$$\{H_{0m}; H_{1m}; H_{2m}\} WW = 2M_{Wc}^2 / v_0 \times \{\cos \theta_{01} \cos \theta_{02}; -\sin \theta_{01} \cos \theta_{02}; -\sin \theta_{02}\}. \quad (3.8)$$

The coupling to Z -boson pairs is more involved if the kinetic mixing modifies the current Z eigenstates to mass

eigenstates as discussed later.

In the same way as above, the triple Higgs couplings in the potential can be derived from the triple Higgs couplings of the mass eigenfields which are accessible, in principle, from experimental data of multiple Higgs production cross sections; in self-explaining notation for small mixing:

$$t_{000}^m \simeq \frac{M_{0m}^2}{2v_0} \cos^3 \theta_{01} \cos^3 \theta_{02} \quad (3.9)$$

$$t_{001}^m \simeq \frac{(2M_{0m}^2 + M_{1m}^2)}{6} \left(\frac{\sin \theta_{01}}{v_1} - \frac{1}{v_0} \right) \quad \text{and} \quad \{1 \leftrightarrow 2\} \quad (3.10)$$

$$t_{011}^m \simeq \frac{(M_{0m}^2 + 2M_{1m}^2)}{6} \left(\frac{\sin \theta_{01}}{v_0} + \frac{1}{v_1} \right) \quad \text{and} \quad \{1 \leftrightarrow 2\} \quad (3.11)$$

$$t_{012}^m \simeq \frac{(M_{0m}^2 + M_{1m}^2 + M_{2m}^2)}{6v_0} \sin \theta_{01} \sin \theta_{02} \quad (3.12)$$

$$t_{111}^m \simeq \frac{M_{1m}^2}{2v_1} \cos^3 \theta_{01} \quad \text{and} \quad \{1 \leftrightarrow 2\} \quad (3.13)$$

$$t_{112}^m \simeq \frac{M_{0m}^2(2M_{1m}^2 + M_{2m}^2)}{6(M_{1m}^2 - M_{2m}^2)v_1} \sin \theta_{01} \sin \theta_{02} \quad \text{and} \quad \{1 \leftrightarrow 2\} \quad (3.14)$$

symmetric under permutations of the Higgs indices.

Thus, three Higgs masses, the couplings of the Higgs bosons to SM pairs and the triple Higgs couplings allow the determination of the current parameters in the Higgs potential.

3.2. Kinetic Mixing

The mixing in the gauge sector can be illustrated in a similar fashion. Disregarding potential mixing of the two abelian gauge fields $V_{1,2}$ within the hidden sector [which could be implemented with no problem], the kinetic mixing of the hypercharge B -field with the abelian gauge fields, and its weak mixing with the neutral $SU(2)$ W -field, affect masses and couplings of the mass vector-eigenstates.

The 2×2 KT matrix σ introduced in Eq. (1.22) is diagonalized by the orthogonal matrix

$$u = \begin{pmatrix} \cos \phi & \sin \phi \\ -\sin \phi & \cos \phi \end{pmatrix} = \frac{1}{|s|} \begin{pmatrix} s_1 & s_2 \\ -s_2 & s_1 \end{pmatrix} \quad (3.15)$$

with $|s| = (s_1^2 + s_2^2)^{1/2}$ for $s = (s_1, s_2)$. The KT matrix σ turns into a diagonal matrix $\text{diag}[\sigma', 1]$ with $\sigma' = (1 - |s|^2)^{-\frac{1}{2}}$. The \mathcal{Z} matrix, transforming the current gauge vector fields $\{W, B, V_1, V_2\}_c$ to the mass vector fields $\{A, Z, V_1, V_2\}_m$ is given by

$$\mathcal{Z} = \begin{pmatrix} s_W & c_W & 0 & 0 \\ c_W & -s_W & 0 & 0 \\ 0 & -(\sigma'^2 - 1)^{1/2} c_\phi & \sigma' c_\phi^2 + s_\phi^2 & (\sigma' - 1) c_\phi s_\phi \\ 0 & -(\sigma'^2 - 1)^{1/2} s_\phi & (\sigma' - 1) c_\phi s_\phi & \sigma' s_\phi^2 + c_\phi^2 \end{pmatrix} \simeq \begin{pmatrix} s_W & c_W & 0 & 0 \\ c_W & -s_W & 0 & 0 \\ 0 & -s_1 & 1 + s_1^2/2 & s_1 s_2/2 \\ 0 & -s_2 & s_1 s_2/2 & 1 + s_2^2/2 \end{pmatrix} \quad (3.16)$$

up to the second order of the mixing $|s|$, with the abbreviations $c_\phi = \cos \phi = s_1/|s|$, etc. The \mathcal{Z} matrix affects the vector-boson masses and the charges when varying the KT factor σ' and the angle ϕ in the mixing column vector s .

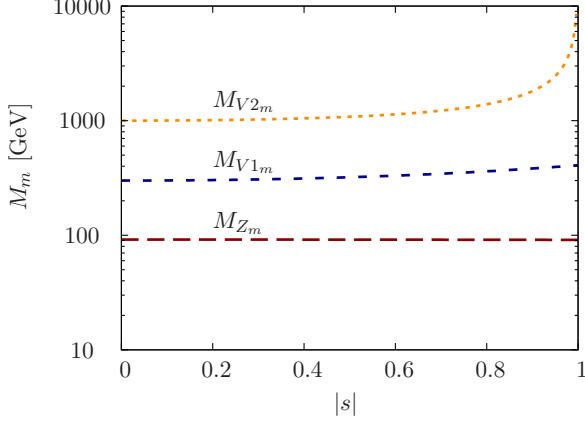


FIG. 8a: Exact V_m and Z_m masses as a function of $|s|$ for $M_{V_{1c}}, M_{V_{2c}} = 300, 1000$ GeV.

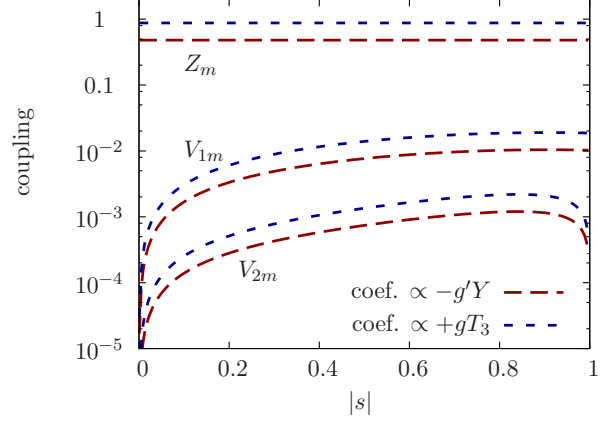


FIG. 8b: Exact V_m and Z_m couplings as a function of $|s|$ for $M_{V_{1c}}, M_{V_{2c}} = 300, 1000$ GeV.

For a small mixing parameter $|s| \ll 1$, the three massive gauge boson masses, in addition to a vanishing photon mass $M_{A_m} = 0$, are given approximately by

$$M_{Z_m}^2 = M_{Z_c}^2 \quad (3.17)$$

$$M_{V_{1m}}^2 = M_{V_{1c}}^2 + M_{V_{1c}}^2 s_1^2 \quad (3.18)$$

$$M_{V_{2m}}^2 = M_{V_{2c}}^2 + M_{V_{2c}}^2 s_2^2 \quad (3.19)$$

up to the second order in the mixing. By construction, the isospin T_3 and hypercharge Y are not changed *a priori* to leading order, while the generalized V charges can be derived from the transformed covariant derivative

$$T_3 W_c \Rightarrow s_W T_3 A_m + c_W T_3 Z_m \quad (3.20)$$

$$Y B_c \Rightarrow c_W Y A_m - s_W Y Z_m \quad (3.21)$$

$$Y_{V_1} V_{1c} + Y_{V_2} V_{2c} \Rightarrow (Y_{V_1} - [g'/g_V] Y s_1) V_{1m} + (Y_{V_2} - [g'/g_V] Y s_2) V_{2m} \quad (3.22)$$

to leading order in the mixing.

The exact mass eigenvalues of V_m are illustrated in Fig. 8a as a function of the kinetic mixing parameters $|s|$ and $\cos \phi = 1/\sqrt{2}$. The charge components correspondingly in Fig. 8b for couplings g_V/g' and $Y_V/Y \Rightarrow 1$.

The $|s|$ -dependence in these figures is easy to understand. For large enough $|s| \rightarrow 1$ the 4×4 mass matrix approaches the limit of two 2×2 system with only weak coupling. The masses in the hidden sector grow for $|s| \rightarrow 1$, leading to strong $|s|$ dependence of the heavier hidden mass eigenvalue as a consequence of the diagonalization of the hidden 2×2 symmetric submatrix. The coefficient $(1 - |s|^2)^{-1}$ approximately cancels for the lighter eigenvalue. The cross-talk of the visible and the hidden sector gives rise to a larger overlap of the light hidden state with the visible sector. Since the V_{2m} is orthogonal to V_{1m} the overlap of the former state with the visible sector becomes minimal in the limit where mixing in the hidden sector dominates for $|s| \rightarrow 1$. In this limit the coupling of V_{1m} to SM matter saturates, while V_{2m} decouples.

The intertwining of the SM and hidden sectors may be illustrated by noting the diagonal Higgs-vector couplings

$$H_{0m} W W / Z_m Z_m = \frac{2M_{W_c/Z_c}^2}{v_0} \cos \theta_{01} \cos \theta_{02} \quad (3.23)$$

$$H_{0m} V_{1m} V_{1m} / V_{2m} V_{2m} = \frac{2M_{Z_c}^2 s_W^2}{v_0} \sigma'^2 |s|^2 \cos \theta_{01} \cos \theta_{02} \cos^2 \phi / \sin^2 \phi \quad (3.24)$$

and the non-diagonal Higgs-vector couplings

$$H_{0m}Z_mV_{1m}/Z_mV_{2m} = \frac{2M_{Z_c}^2 s_W}{v_0} \sigma' |s| \cos \theta_{01} \cos \theta_{02} \cos \phi / \sin \phi \quad (3.25)$$

$$H_{0m}V_{1m}V_{2m} = \frac{M_{Z_c}^2 s_W^2}{v_0} \sigma'^2 |s|^2 \cos \theta_{01} \cos \theta_{02} \sin 2\phi \quad (3.26)$$

in which the W couplings are modified only by Higgs mixing while the Z_m and $V_{1m,2m}$ couplings are affected by the superposition of Higgs and vector mixings.

4. SUMMARY

In this report we have taken a first modest step in analyzing scenarios in which the SM is coupled to a hidden sector comprising more than one degree of freedom. The difficulty of the analysis rises enormously with the complexity of the hidden sector that can only be accessed through mixing effects with the SM fields. The simplest structures of the hidden sector are abelian or [extended] SM-type gauge theories broken by the Higgs mechanism. The Higgs fields interact with the SM Higgs field by means of bilinear quartic couplings, the vector fields by means of kinetic mixing with the SM hypercharge field.

In the first part we have analyzed quite generally the mixing effects within the Higgs system and within the vector system for an arbitrary number of degrees of freedom. Closed and transparent analytical solutions can only be obtained for $1 \oplus 1$ configurations. Approximate solutions however can be obtained quite generally to leading non-trivial order of small mixings. In the Higgs as well as gauge sector the mass matrix can systematically be diagonalized to arbitrary order.

Two examples illustrate the abstract analysis. For the $1 \oplus 1$ system we have studied a complete set of observables which allow to reconstruct the set of fundamental parameters in the Lagrangian, in principle. Higgs and vector-boson masses and their trilinear couplings, supplemented by fermion couplings, generate such an ensemble. Since all the Higgs and vector-boson states which are identified experimentally, are mixed mass eigenstates, the effective vertices are complicated mixtures in which Higgs mixing and kinetic mixing are intertwined. If the mixing is too small the associated cross sections may, partly, not be large enough to measure the vertices involved, but blocks of essential elements in the Lagrangian can nevertheless be isolated.

Precision analyses of the electroweak sector allow to constrain the $1 \oplus 1$ system at present and future colliders. Direct detection limits at the LHC in Drell-Yan type production will give upper production limits on the additional neutral vector boson. Other channels like WW production and the search for anomalous ZWW interactions will (and in fact already do) constrain the associated mixing via modifying the SM coupling pattern, resulting in a phenomenology sensitive to the described coupling modifications. A precise measurement of the Higgs self-interaction facilitates a complete determination of the extended Higgs-sector parameters. Current extrapolations suggest that only a lower limit on the hidden-sector vacuum expectation value can be established. The potentially clean environment of a lepton collider, however, might be able to amend this conservative statement at high luminosity.

The study has been extended to the system in which the SM interacts with a hidden sector comprising two Higgs and vector-boson degrees of freedom. It could be shown that for small mixing, in addition to the numerical evaluation, this system also can be analyzed analytically. Furthermore, the measurement strategies that we have outlined in Sec. 2 can be directly generalized to the $1 \oplus 2$ analysis. The situation, however, becomes less transparent due to the increase in parameters while the number of phenomenologically accessible measurements [especially in the

Higgs sector where large mixing effects could be present] stays the same.

In toto. If the Standard Model is coupled weakly to a complex hidden sector, essential elements of this novel sector can be reconstructed, though the experimental analysis may turn out very difficult, and partly incomplete, if mixings are too small.

APPENDIX

A. Mixing in the Hidden Sector

If quartic [bi-bilinear] mixing terms in the hidden sector are included, the Higgs potential is generalized to

$$\begin{aligned} \mathcal{V}_{\mathcal{H}} &= \sum_{i=0}^n [\mu_i^2 |S_i|^2 + \lambda_i |S_i|^4] + \frac{1}{2} \sum_{i \neq j=0}^n \eta_{ij} |S_i|^2 |S_j|^2 \\ &= [\mu^{2T} |S|^2 + |S|^{2T} \lambda |S|^2] + \frac{1}{2} |S|^{2T} \eta |S|^2 \end{aligned} \quad (\text{A.1})$$

in obvious vector/matrix notation in the second row. The index $i = 0$ represents the Higgs field in the SM sector, i.e. $S_0 = \phi$ and $\eta_{0j} = \eta_j$ [$j = 1, \dots, n$] etc, while indices $j \geq 1$ refer to hidden-sector scalar fields.

The visible and hidden components v of the vacuum Higgs fields are defined by the vanishing of the derivative of the Higgs potential,

$$\begin{aligned} v^2 &= -\{\lambda + \frac{1}{2}\eta\}^{-1} \mu^2 \\ &\simeq -\{\lambda^{-1} - \frac{1}{2}\lambda^{-1}\eta\lambda^{-1}\} \mu^2 \end{aligned} \quad (\text{A.2})$$

for small off-diagonal mixing parameters η and $\mathcal{O}(1)$ diagonal parameters λ .

The term bilinear in the physical fields defines the masses of the Higgs particles,

$$\begin{aligned} \mathcal{M}_H^2 &= 2v^T \{\lambda + \frac{1}{2}\eta\} v \\ &= \begin{pmatrix} 2\lambda_0 v_0^2 & \eta_1 v_0 v_1 & \eta_2 v_0 v_2 & \cdots & \eta_n v_0 v_n \\ & 2\lambda_1 v_1^2 & \eta_{12} v_1 v_2 & \cdots & \eta_{1n} v_1 v_n \\ \{ \text{symmetric} \} & & \ddots & & \vdots \\ & & & & 2\lambda_n v_n^2 \end{pmatrix} \end{aligned} \quad (\text{A.3})$$

Restricting the $n \times n$ symmetric mass matrix M_c^2 to the components of the hidden sector in the notation of Eq. (1.7), the matrix can be diagonalized by an orthogonal transformation \mathcal{O}_c , modifying subsequently the phenomenological mixing vector X in Eq. (1.8):

$$\begin{aligned} M_c^2 &\rightarrow M_{c/\text{diag}}^2 = \mathcal{O}_c M_c^2 \mathcal{O}_c^T \\ X &\rightarrow \mathcal{O}_c X. \end{aligned} \quad (\text{A.4})$$

Notice that the off-diagonal \mathcal{O}_c mixing elements change X only to higher order so that the portal interactions between visible and hidden sector fields are essentially not affected by the quartic mixing in the hidden sector.

Finally, the self-interactions among the Higgs fields, SM and hidden, can be derived from the potential

$$\mathcal{V}_{\mathcal{H}/\text{self}} = \{\lambda + \frac{1}{2}\eta\}_{ij} [v_i H_{ic} H_{jc}^2 + \frac{1}{4} H_{ic}^2 H_{jc}^2] \quad (\text{A.5})$$

in terms of the physical Higgs fields in the current [c] representation.

B. Dyadic Matrix

It is straightforward to diagonalize the $n \times n$ dyadic matrix D formed by a n -dimensional column vector $x = (x_1, \dots, x_n)^T$ and its transpose x^T as

$$D_{ij} = (xx^T)_{ij} = x_i x_j. \quad (\text{B.6})$$

Making use of the rules for calculating determinants, one eigenvalue emerges as positive and the other $(n - 1)$ eigenvalues as zero:

$$d_1 = \sum_{i=1}^n x_i^2 \quad \text{and} \quad d_j = 0 \quad [j = 2 \text{ to } n]. \quad (\text{B.7})$$

The eigenvectors associated with the eigenvalues read

$$v_1 = d_1^{-1/2} x, \quad \text{and} \quad v_{j=2, \dots, n} \text{ orthogonal to } v_1 \quad (\text{B.8})$$

normalized to unity.

C. Block-diagonalization : Higgs and Vector Masses

1.) The eigen-masses and mixings in the Higgs sector, when block-diagonalizing the real and symmetric matrix $\mathcal{M}^2 \Rightarrow \mathcal{M}_m^2$ by an orthogonal transformation \mathcal{O} ,

$$\mathcal{M}^2 = \begin{pmatrix} M_0^2 & X^T \\ X & M^2 \end{pmatrix} = \begin{pmatrix} 0 & 0 \\ 0 & M^2 \end{pmatrix} + \begin{pmatrix} M_0^2 & X^T \\ X & 0 \end{pmatrix} \quad \Rightarrow \quad \mathcal{M}_m^2 = \mathcal{O} \mathcal{M}^2 \mathcal{O}^T = \begin{pmatrix} \hat{M}_0^2 & 0 \\ 0 & \hat{M}^2 \end{pmatrix} \quad (\text{C.1})$$

can iteratively be constructed from the lowest order to arbitrary order in the expansion parameter $\epsilon \sim \|M_0^2\|/\|M^2\|, \|X\|/\|M^2\|$. The first, large part of the mass matrix will be called \mathcal{M}_0^2 , the second, small part \mathcal{E} which is order ϵ compared with \mathcal{M}_0^2 . Thus, the expansion is valid for masses in the hidden sector large compared to SM masses and the mixings.

The conditions which determine the mixing matrix \mathcal{O} for block-diagonalization of the mass matrix \mathcal{M}^2 are orthogonality and diagonality:

$$\mathcal{O} = \sum_{N=0}^{\infty} o_N \quad \text{with} \quad o_0 = 1 \quad \text{and} \quad o_N \sim \epsilon^N \quad (\text{C.2})$$

$$\mathcal{M}_m^2 = \begin{pmatrix} 0 & 0 \\ 0 & M^2 \end{pmatrix} + \begin{pmatrix} M_0^2 & 0 \\ 0 & 0 \end{pmatrix} + \sum_{N=2}^{\infty} \begin{pmatrix} \hat{M}_{0,N}^2 & 0 \\ 0 & \hat{M}_N^2 \end{pmatrix} \quad (\text{C.3})$$

The first two matrices in \mathcal{M}_m^2 will occasionally be identified with indices $j = 0$ and 1, respectively.

(i) The *orthogonality* condition for \mathcal{O} determines the symmetric part of the component o_N from $o_{j < N}$ as

$$o_N + o_N^T = - \sum_{j=1}^{N-1} o_j o_{N-j}^T. \quad (\text{C.4})$$

(ii) The *diagonalization* condition of the mass matrix determines the antisymmetric part of o_N from the off-diagonal block elements, and at the same time the expansion of the mass eigenvalues from the diagonal block elements:

$$\begin{pmatrix} \hat{M}_{0,N}^2 & 0 \\ 0 & \hat{M}_N^2 \end{pmatrix} = \sum_{j=0}^N o_j \mathcal{M}_0^2 o_{N-j}^T + \sum_{j=0}^{N-1} o_j \mathcal{E} o_{N-1-j}^T \quad \text{with} \quad \mathcal{M}_0^2 = \begin{pmatrix} 0 & 0 \\ 0 & M^2 \end{pmatrix} \quad \text{and} \quad \mathcal{E} = \begin{pmatrix} M_0^2 & X^T \\ X & 0 \end{pmatrix} \quad (\text{C.5})$$

for $N \geq 1$.

To simplify the notation we switch from indexed symbols to one-letter symbols by denoting

$$o_N = \begin{pmatrix} x_N & y_N^T \\ -y_N & z_N \end{pmatrix}. \quad (\text{C.6})$$

The matrix $z = z^T$ is taken symmetric, the antisymmetric part of o_N is defined in the y column and row. To unify the mass dimensions and express all the formulae in compact form, we introduce three dimensionless and two dimensionful matrices as

$$\begin{aligned} \mu &= M^{-2}M_0^2 & y_{(N)+} &= M^2y_{(N)} \\ y &= M^{-2}X & y_{(N)-} &= M^{-2}y_{(N)} \\ \hat{z}_N &= M^{-2}z_NM^2 \end{aligned} \quad (\text{C.7})$$

where y_{\pm} however always come as dimensionless combinations.

The simplified recurrence relations of the matrix blocks may be cast in the following form for the block-diagonal components:

$$\begin{aligned} x_0 &= 1 & z_0 &= 1 \\ x_1 &= 0 & z_1 &= 0 \\ x_2 &= -\frac{1}{2}y^T y & z_2 &= -\frac{1}{2}yy^T \\ x_3 &= -y^T \mu y & z_3 &= -\frac{1}{2}\{yy^T, \mu\} \\ &\vdots & &\vdots \\ x_N &= -\frac{1}{2}\sum_{j=1}^{N-1} (x_j x_{N-j} + y_j^T y_{N-j}) & z_N &= -\frac{1}{2}\sum_{j=1}^{N-1} (z_j z_{N-j} + y_j y_{N-j}^T) \end{aligned} \quad (\text{C.8})$$

and for the off-diagonal components:

$$\begin{aligned} y_0 &= 0, & y_1 &= -y, & y_2 &= -\mu y, & y_3 &= -\mu^2 y - \frac{1}{2}(y^T y y - y_+^T y y_-) \\ &\vdots & & & & & & \\ y_N &= \sum_{j=0}^{N-1} \{ (\mu y_j - \hat{z}_j y) x_{N-1-j} - \hat{z}_{N-j} y_j + y_+^T y_{N-1-j} y_{j-} \}. \end{aligned} \quad (\text{C.9})$$

The block-diagonal components of the mass matrix \mathcal{M}_m^2 are given by

$$\begin{aligned} \hat{M}_{0,0}^2 &= 0 & \hat{M}_{0,1}^2 &= M_0^2 & \hat{M}_{0,2}^2 &= -y^T M^2 y & \hat{M}_{0,3}^2 &= -M_0^2 y^T y \\ \hat{M}_0^2 &= M^2 & \hat{M}_1^2 &= 0 & \hat{M}_2^2 &= \frac{1}{2}\{yy^T, M^2\} & \hat{M}_3^2 &= M_0^2 yy^T \\ &\vdots & & & & & & \\ \hat{M}_{0,N}^2 &= \sum_{j=0}^N y_j^T M^2 y_{N-j} + \sum_{j=0}^{N-1} [M_0^2 x_j x_{N-1-j} + (y_j^T X + X^T y_j) x_{N-1-j}] \\ \hat{M}_N^2 &= \sum_{j=0}^N z_j M^2 z_{N-j} + \sum_{j=0}^{N-1} [M_0^2 y_j y_{N-1-j}^T - (z_j X y_{N-1-j}^T + y_{N-1-j} X^T z_j)] . \end{aligned} \quad (\text{C.10})$$

2.) In the same way the mass matrix in the gauge sector can be diagonalized recursively for small gauge-kinetic

mixing s . After applying the KT matrix \mathcal{Z} , given in closed form by

$$\mathcal{Z} = \begin{pmatrix} s_W & c_W & 0 \\ c_W & -s_W & 0 \\ 0 & -\sigma s & \sigma \end{pmatrix} \quad (\text{C.11})$$

with the symmetric matrix $\sigma = (1 - ss^T)^{-1/2}$, the transformed $(2+n) \times (2+n)$ mass matrix

$$\mathcal{M}_s^2 = \mathcal{Z} \mathcal{M}_c^2 \mathcal{Z}^T = M_{Z_c}^2 \begin{pmatrix} 0 & 0 & 0 \\ 0 & 1 & s_W s^T \sigma \\ 0 & s_W \sigma s & \sigma(\Delta + s_W^2 s s^T) \sigma \end{pmatrix} \quad \text{with} \quad \Delta = M_{V_c}^2 / M_{Z_c}^2 \quad (\text{C.12})$$

has the characteristic properties which allow the recursive diagonalization according to the algorithm developed in the previous subsection. Disregarding the photonic null-vectors, we can identify, in symbolic notation,

$$M_0^2 \sim M_{Z_c}^2; \quad M^2 \sim M_{V_c}^2; \quad X \sim M_{Z_c}^2 s \quad (\text{C.13})$$

for the $(1+n) \times (1+n)$ mass submatrix with $\|M^2\| \gg M_0^2 \gg \|X\|$. However, the kinetic mass matrix includes additional s -dependent terms which can be expanded for small s . They add contributions $\Sigma \mathcal{E}^k$ to the matrix \mathcal{E} in Eq.(C.5). Since they affect the matrix o_N only by already known matrices $o_{j < N-1}$, they are easy to incorporate. This procedure is straightforward, though technically cumbersome, and we will not present the additional terms in detail.

D. Re-diagonalization

After the block-diagonalization the mass matrix $\hat{M}^2 = M^2 + \Delta$ in the hidden sector is not diagonal anymore. Here, the correction term Δ is of the second order or higher in ϵ . It may be re-diagonalized $\hat{M}^2 \rightarrow [\text{diag } \hat{M}^2] = M^2 + \Delta^d$ by the orthogonal transformation $U = 1 + u$. Expanding all the matrices, $\Delta^{(d)} = \sum \Delta_N^{(d)}$ and $u = \sum u_N$, systematically in terms of the power $N \geq 2$ of ϵ , the diagonal mass matrix and the orthogonal transformation matrix can easily be constructed recursively, as worked out before.

The *orthogonality* condition determines the symmetric part of u_N in terms of the predetermined lower-order matrices $u_{k \leq N-2}$ by the relation

$$u_N + u_N^T = - \sum_{k=2}^{N-2} u_k u_{N-k}^T \quad (\text{D.1})$$

Introducing the symmetric auxiliary matrix

$$A_N = \sum_{k=2}^{N-2} \left[u_k M^2 u_{N-k}^T + (u_{N-k} \Delta_k + \Delta_k u_{N-k}^T) + \sum_{l=2}^{N-2-k} u_k \Delta_l u_{N-k-l}^T \right] \quad (\text{D.2})$$

the *diagonalization* condition

$$\Delta_N^d = \Delta_N + u_N M^2 + M^2 u_N^T + A_N \quad (\text{D.3})$$

can be exploited to project out the antisymmetric part of u_N ,

$$[u_N - u_N^T]_{ab} = 2I_{ab} \left[\Delta_{N ab} + \frac{1}{2}(M_{aa}^2 + M_{bb}^2)[u_N + u_N^T]_{ab} + A_{N ab} \right] \quad [a \neq b] \quad (\text{D.4})$$

with the abbreviation $I_{ab} = 1/(M_{aa}^2 - M_{bb}^2)$ and the symmetric part calculated before by means of the orthogonality condition. The diagonalized eigenvalues are given by the elements of the matrix Δ_N^d in Eq. (D.2), which, at this point, includes only predetermined matrices u_N, A_N on the right-hand side. In this way the re-diagonalization of the mass matrix in the hidden sector is completed.

These solutions may be illustrated for the first three non-trivial cases. The second- and third-order terms read

$$N = 2, 3 : \quad \Delta_{2,3 aa}^d = \Delta_{2,3 aa} \quad (\text{D.5})$$

$$u_{2,3 aa} = 0 \quad (\text{D.6})$$

$$u_{2,3 ab} = I_{ab} \Delta_{2,3 ab} \quad [a \neq b]. \quad (\text{D.7})$$

The transformation matrix $u_{2,3}$ is apparently antisymmetric. As a result, the newly diagonalized mass matrix in the hidden sector is found by just truncating the mass matrix after block-diagonalization to the diagonal elements up to the third order. However, starting from the fourth order, there appear non-trivial contributions to the diagonal elements from the lower-order terms. The fourth-order terms read

$$N = 4 : \quad \Delta_{4 aa}^d = \Delta_{4 aa} + \sum_{c \neq a} I_{ac} \Delta_{2 ac}^2 \quad (\text{D.8})$$

$$u_{4 aa} = -\frac{1}{2} \sum_{c \neq a} I_{ac}^2 \Delta_{2 ac}^2 \quad (\text{D.9})$$

$$u_{4 ab} = I_{ab} \Delta_{4 ab} - I_{ab}^2 \Delta_{2 aa} \Delta_{2 ab} + \sum_{c \neq a} I_{ab} I_{ac} \Delta_{2 ac} \Delta_{2 bc} \quad [a \neq b]. \quad (\text{D.10})$$

Note that the fourth-order matrix u_4 is not antisymmetric any more.

Acknowledgements

C.E. thanks Joerg Jaeckel, Valya Khoze and Michael Spannowsky for helpful discussions. The work of S.Y.C. was supported by Basic Science Research Program through the National Research Foundation (NRF) funded by the Ministry of Education, Science and Technology (NRF-2011-0010835).

-
- [1] P. A. R. Ade *et al.* [Planck Collaboration], arXiv:1303.5076 [astro-ph.CO].
 - [2] J. Fan, A. Katz, L. Randall and M. Reece, Phys. Rev. Lett. **110** (2013) 211302; J. Fan, A. Katz, L. Randall and M. Reece, arXiv:1303.1521 [astro-ph.CO]; M. McCullough and L. Randall, arXiv:1307.4095 [hep-ph].
 - [3] R. Schabinger and J. D. Wells, Phys. Rev. D **72** (2005) 093007; B. Patt and F. Wilczek, hep-ph/0605188; M. Bowen, Y. Cui and J. D. Wells, JHEP **0703** (2007) 036; S. Chang, R. Dermisek, J. F. Gunion and N. Weiner, Ann. Rev. Nucl. Part. Sci. **58** (2008) 75; J. D. Wells, In *Kane, Gordon (ed.), Pierce, Aaron (ed.): Perspectives on LHC physics* 283-298 [arXiv:0803.1243 [hep-ph]].
 - [4] E. Weihs and J. Zurita, JHEP **1202** (2012) 041.
 - [5] R. Foot, H. Lew and R. R. Volkas, Phys. Lett. B **272** (1991) 67; R. Foot, H. Lew and R. R. Volkas, Mod. Phys. Lett. A **7** (1992) 2567; Z. Chacko, H. -S. Goh and R. Harnik, Phys. Rev. Lett. **96** (2006) 231802; Y. G. Kim, K. Y. Lee and S. Shin, JHEP **0805** (2008) 100; M. Kadastik, K. Kannike and M. Raidal, Phys. Rev. D **81** (2010) 015002; T. Hur and P. Ko, Phys. Rev. Lett. **106** (2011) 141802; O. Lebedev and H. M. Lee, Eur. Phys. J. C **71** (2011) 1821; J. -W. Cui, H. -J. He, L. -C. Lu and F. -R. Yin, Phys. Rev. D **85** (2012) 096003; A. Djouadi, O. Lebedev, Y. Mambrini and J. Quevillon, Phys. Lett. B **709** (2012) 65; N. Desai, B. Mukhopadhyaya and S. Niyogi, arXiv:1202.5190 [hep-ph]; L. Lopez-Honorez, T. Schwetz and J. Zupan, Phys. Lett. B **716** (2012) 179; S. Baek, P. Ko and W. -I. Park, JHEP **1202** (2012) 047; C. Englert, J. Jaeckel, V. V. Khoze and M. Spannowsky, JHEP **1304** (2013) 060; M. Heikinheimo, A. Racioppi, M. Raidal, C. Spethmann and K. Tuominen, arXiv:1304.7006 [hep-ph]; S. Baek, P. Ko, W. -I. Park and E. Senaha, JHEP **1305** (2013) 036; V. V. Khoze

- and G. Ro, arXiv:1307.3764 [hep-ph]; S. Baek, P. Ko and W. -I. Park, JHEP **1307** (2013) 013; M. Heikinheimo, A. Racioppi, M. Raidal and C. Spethmann, arXiv:1307.7146 [hep-ph].
- [6] G. Buchalla, O. Cata and C. Krause, arXiv:1307.5017 [hep-ph]; G. Buchalla and O. Cata, JHEP **1207** (2012) 101.
- [7] J. R. Andersen, M. Rauch and M. Spannowsky, arXiv:1308.4588 [hep-ph].
- [8] B. Holdom, Phys. Lett. B **166** (1986) 196.
- [9] L. B. Okun, Sov. Phys. JETP **56** (1982) 502; Zh. Eksp. Teor. Fiz. **83** (1983) 892; K. R. Dienes, C. F. Kolda and J. March-Russell, Nucl. Phys. B **492** (1997) 104; M. Ahlers, H. Gies, J. Jaeckel, J. Redondo and A. Ringwald, Phys. Rev. D **76** (2007) 115005; S. A. Abel, M. D. Goodsell, J. Jaeckel, V. V. Khoze and A. Ringwald, JHEP **0807** (2008) 124; C. Cheung, J. T. Ruderman, L. -T. Wang and I. Yavin, Phys. Rev. D **80** (2009) 035008; K. L. McDonald and D. E. Morrissey, JHEP **1005** (2010) 056; M. Cicoli, M. Goodsell, J. Jaeckel and A. Ringwald, JHEP **1107** (2011) 114; A. Hook, E. Izaguirre and J. G. Wacker, Adv. High Energy Phys. **2011** (2011) 859762; E. J. Chun, J. -C. Park and S. Scopel, JHEP **1102** (2011) 100; J. Heeck and W. Rodejohann, Phys. Lett. B **705** (2011) 369; M. T. Frandsen, F. Kahlhoefer, A. Preston, S. Sarkar and K. Schmidt-Hoberg, JHEP **1207** (2012) 123.
- [10] C. Englert, T. Plehn, D. Zerwas and P. M. Zerwas, Phys. Lett. B **703** (2011) 298.
- [11] M. Goodsell, J. Jaeckel, J. Redondo and A. Ringwald, JHEP **0911** (2009) 027.
- [12] R. Barbieri, T. Gregoire and L. J. Hall, hep-ph/0509242.
- [13] S. Y. Choi, D. J. Miller and P. M. Zerwas, Nucl. Phys. B **711** (2005) 83; S. Y. Choi, H. E. Haber, J. Kalinowski and P. M. Zerwas, Nucl. Phys. B **778** (2007) 85.
- [14] S. Bock, R. Lafaye, T. Plehn, M. Rauch, D. Zerwas and P. M. Zerwas, Phys. Lett. B **694** (2010) 44; G. Guo, B. Ren and X. -G. He, arXiv:1112.3188 [hep-ph]; B. Batell, S. Gori and L. -T. Wang, JHEP **1206** (2012) 172; D. Bertolini and M. McCullough, JHEP **1212** (2012) 118; B. Batell, D. McKeen and M. Pospelov, JHEP **1210** (2012) 104.
- [15] M. E. Peskin and T. Takeuchi, Phys. Rev. Lett. **65** (1990) 964; Phys. Rev. D **46** (1992) 381.
- [16] M. Klute, R. Lafaye, T. Plehn, M. Rauch and D. Zerwas, Europhys. Lett. **101** (2013) 51001.
- [17] B. A. Dobrescu and J. D. Lykken, JHEP **1302** (2013) 073.
- [18] M. J. Dolan, C. Englert and M. Spannowsky, Phys. Rev. D **87** (2013) 055002.
- [19] E. W. N. Glover and J. J. van der Bij, Nucl. Phys. B **309** (1988) 282; D. A. Dicus, C. Kao and S. S. D. Willenbrock, Phys. Lett. B **203** (1988) 457; T. Plehn, M. Spira and P. M. Zerwas, Nucl. Phys. B **479** (1996) 46 [Erratum-ibid. B **531** (1998) 655]; S. Dawson, S. Dittmaier and M. Spira, Phys. Rev. D **58** (1998) 115012; A. Djouadi, W. Kilian, M. Muhlleitner and P. M. Zerwas, Eur. Phys. J. C **10** (1999) 45; A. Papaefstathiou, L. L. Yang and J. Zurita, Phys. Rev. D **87** (2013) 011301; J. Baglio, A. Djouadi, R. Gröber, M. M. Mühlleitner, J. Quevillon and M. Spira, JHEP **1304** (2013) 151; F. Goertz, A. Papaefstathiou, L. L. Yang and J. Zurita, JHEP **1306** (2013) 016.
- [20] The ATLAS Collaboration, ATL-PHYS-PUB-2012-004.
- [21] M. J. Dolan, C. Englert and M. Spannowsky, JHEP **1210** (2012) 112.
- [22] U. Baur, T. Plehn and D. L. Rainwater, Phys. Rev. D **69** (2004) 053004.
- [23] A. Djouadi, W. Kilian, M. Muhlleitner and P. M. Zerwas, Eur. Phys. J. C **10** (1999) 27.
- [24] Y. Takubo, arXiv:0907.0524 [hep-ph]; J. Tian, K. Fujii and Y. Gao, arXiv:1008.0921 [hep-ex].
- [25] The ATLAS Collaboration, ATLAS-CONF-2012-007.
- [26] S. Chatrchyan *et al.* [CMS Collaboration], Phys. Lett. B **714** (2012) 158.
- [27] B. Holdom, Phys. Lett. B **259** (1991) 329.
- [28] G. Aad *et al.* [ATLAS Collaboration], Phys. Rev. D **87** (2013) 112001 [arXiv:1210.2979 [hep-ex]].
- [29] S. Chatrchyan *et al.* [CMS Collaboration], arXiv:1306.1126 [hep-ex].
- [30] S. Schael *et al.* [ALEPH and DELPHI and L3 and OPAL and LEP Electroweak Working Group Collaborations], arXiv:1302.3415 [hep-ex].
- [31] S. J. Brodsky and R. W. Brown, Phys. Rev. Lett. **49** (1982) 966; R. W. Brown, K. L. Kowalski and S. J. Brodsky, Phys. Rev. D **28**, 624 (1983).
- [32] J. Jaeckel, M. Jankowiak and M. Spannowsky, Phys. Dark Univ. **2** (2013) 111.
- [33] S. T. Boogert and D. J. Miller, hep-ex/0211021.